


## Entropy fluctuation and correlation transfer in tunable discrete-time quantum walk with fractional Gaussian noise

S. V. Muniandy<sup>1,\*</sup>, Nur Izzati Ishak<sup>1</sup> and Chong Wu Yi<sup>2</sup>

<sup>1</sup>*Center for Theoretical and Computational Physics, Department of Physics, Faculty of Science, University of Malaya, Kuala Lumpur 50603, Malaysia*

<sup>2</sup>*Photonics Research Centre, University of Malaya, Kuala Lumpur 50603, Malaysia*

 (Received 3 February 2022; accepted 26 July 2022; published 15 August 2022)

We study the time correlation in the von Neumann entropy fluctuation of the tunable discrete-time quantum walk in one dimension, induced by the coin disorder arising from the temporal fractional Gaussian noise (fGn). The fGn is characterized by the Hurst exponent  $H$ , which provides three different correlation scenarios, namely antipersistent ( $0 < H < 0.5$ ), memoryless ( $H = 0.5$ ), and persistent ( $0.5 < H < 1$ ). We show the correlation of fGn is transferred to the coin's degree of entanglement and eventually transpires in the time correlation of the von Neumann entropy fluctuation. This study hints at the potential of using noise correlation as a resource to sustain information backflow via the interaction of quantum system with the noisy environment.

DOI: [10.1103/PhysRevE.106.024113](https://doi.org/10.1103/PhysRevE.106.024113)

### I. INTRODUCTION

Information backflow emerges as quantum memory due to the interaction of quantum system with the environment. It is known to be one of the resources in maintaining or protecting the quantum entanglement [1–3]. In the implementation of the quantum algorithm, Dong *et al.* [4] showed the information backflow assisted the high fidelity refined in the Deutsch-Jozsa algorithm with a solid spin in diamond [4]. It is also pointed out in Ref. [5] that the stationary coherence in dephasing qubits is maximized as a direct consequence of information backflow due to reservoir memory effects.

In the bipartite quantum system such as the discrete-time quantum walk (DTQW), Kumar *et al.* [6] suggested information backflow occurs as a result of the interaction of qubit (coin) degree of freedom with the position space, which acts as the environment. This backflow of information can be directly deduced from the oscillation in the time evolution of the von Neumann entropy calculated using the reduced coin (qubit) density matrix. Such behavior is found in both homogeneous [6] and inhomogeneous [6,7] time evolution of the DTQW. Inhomogeneity in time evolution of DTQW can be induced by injecting classical noise, such as uncorrelated noise, leading to an increase in the information backflow [6]. It was also noted that the effect of information backflow in triggering the formation of the weak localization and strong Anderson localization in position space.

Noise is generally considered as source of decoherence in many physical realizations of DTQW. However, noise correlation has also been shown to enhance the transport of coherence logic qubits [8]. Temporal noise can produce a strong memory effect leading to quantum speedup in the walker dynamics [9]. In this study, we investigate the possibility of using classical fractional Gaussian noise (fGn) indexed by the Hurst parameter,  $H$  as a resource for controlling the quantum walk system.

We also demonstrate how the correlation behavior of the fGn is transferred to the quantum walk dynamics, manifested in the fluctuation of the von Neumann entropy. The degree of this correlation transfer is examined for three different regimes of fGn's Hurst parameter, namely antipersistent ( $0 < H < 0.5$ ), memoryless ( $H = 0.5$ ), and persistent ( $0.5 < H < 1$ ), as well as with respect to different noise amplitudes. The paper is organized as follows. In Sec. II, we set up the theoretical framework by introducing the fractional Brownian motion (fBm) and its corresponding derivative process, known as the fractional Gaussian noise, followed by a brief note on the standard discrete-time quantum walk and its generalization to accommodate the temporal fGn noise. Section III describes the simulation procedures of the standard and the noisy DTQW. We present the results in Sec. IV covering the weak localization of the noisy DTQW, information backflow, and how the correlation transfer is deduced from the fluctuation of the entropy. Section V ends with the conclusion that can be drawn from this study.

### II. THEORY

#### A. Fractional Brownian motion and fractional Gaussian noise

Fractional Brownian motion is a self-similar Gaussian process with stationary increments. A widely accepted stochastic representation of fBm was introduced by Mandelbrot and van Ness [10] as given by

$$B_H(t) = \frac{1}{\Gamma(H + \frac{1}{2})} \left( \int_{-\infty}^0 [(t-s)^{H-(1/2)} - (-s)^{H-(1/2)}] \times dB(s) + \int_0^t (t-s)^{H-(1/2)} dB(s) \right), \quad (1)$$

where  $\Gamma$  is the gamma function and  $0 < H < 1$  is the Hurst parameter. Hurst parameter is the measure of self-similarity and  $B_{1/2}(t) = B(t)$  is the standard Brownian

\*msithi@um.edu.my

motion. The normalized fractional Brownian motion  $B_H = \{B_H(t) : 0 \leq t \leq \infty\}$  is characterized by the following properties:

- (i)  $B_H(t)$  has stationary increments;
- (ii)  $B_H(0) = 0$  and  $E[B_H(t)] = 0$  for  $t \geq 0$ ;
- (iii)  $E[B_H^2(t)] = t^{2H}$  for  $t \geq 0$ ; and
- (iv)  $B_H(t)$  has Gaussian distribution for  $t \geq 0$ ,

where  $E$  denotes expectation value. For the continuous sample path of fBm, the covariance function is given by

$$C(s, t) = E[B_H(s)B_H(t)] = \frac{1}{2}\{t^{2H} + s^{2H} - (t-s)^{2H}\} \quad (2)$$

For  $0 < s \leq t$  the incremental process  $W_H = \{W_H(k) : k = 0, 1, \dots\}$  of fBm is given by

$$W_H = B_H(k+1) - B_H(k), \quad (3)$$

and it is called the fractional Gaussian noise (fGn) corresponding to the white-noise counterpart of Brownian motion. The derivative of the fBm (in the generalized sense) produces the corresponding fGn, while the integration of fGn gives the corresponding fBm. It should be noted fGn is the stationary Gaussian process with correlation function given by [11]

$$C(s, t) = \frac{1}{2}[(t-s-1)^{2H} - 2(t-s)^{2H} + (t-s+1)^{2H}], \quad (4)$$

or written using lag time  $\tau = (t-s)$  as

$$C(\tau) = \frac{1}{2}[(\tau+1)^{2H} - 2\tau^{2H} + (\tau-1)^{2H}], \quad (5)$$

and for the large  $\tau$ , (5) can be approximated as

$$C(\tau) = H[(2H-1)\tau^{2H-2}]. \quad (6)$$

Using the power-law correlation property (6), fGn is widely used as a fractal noise model with three different regimes of correlation behavior depending on the value of  $H$  parameter [12–14]. If  $0 < H < 0.5$ , the process has a short-time memory (antipersistent) with a negative correlation, where positive increments in the past are followed by negative increments in the future and vice versa. For  $0.5 < H < 1$ , the process has long-time memory (persistent) with positive correlation, where positive increments in the past are led by positive increments in the future and vice versa. For  $H = 0.5$ , fGn reduces to the standard white noise with zero correlation (uncorrelated).

### B. Standard noiseless discrete-time quantum walk

Discrete-time quantum walk is defined in the composite Hilbert space of  $\mathcal{H} = \mathcal{H}_c \otimes \mathcal{H}_x$  consisting of coin Hilbert space  $\mathcal{H}_c$  with basis of  $\{|0\rangle, |1\rangle\}$  representing the two-dimensional internal degree of freedom of qubit state and the position Hilbert space  $\mathcal{H}_x$  with basis of  $|x\rangle$  that corresponds to the degree of freedom of position-lattice space. One can use the initial wave function of the quantum walk defined as  $|\Psi_0\rangle = 1/\sqrt{2}(|0\rangle + i|1\rangle) \otimes |x=0\rangle$  to represent the symmetric superposition probability amplitude at the initial point of reference. The quantum walk is driven by the single-parameter coin operator  $\hat{C}$  defined as

$$\hat{C} = \begin{bmatrix} \cos(\theta) & \sin(\theta) \\ \sin(\theta) & -\cos(\theta) \end{bmatrix}, \quad (7)$$

with  $0^\circ \leq \theta \leq 90^\circ$ , which only acts on the qubit-state internal degree of freedom in the coin Hilbert space. This coin operator

can be expressed in term of Pauli matrices as  $\hat{C} = e^{-i\theta\hat{n}\sigma}$ , where the direction of the rotation is defined by unit vector  $\hat{n}$ . Here the expression of coin operator in (7) refers to the rotation of the internal state of qubit in the  $x-z$  plane of the Bloch sphere with specific angle  $\theta$ . Then,  $\hat{n} = \hat{n}_y$  with  $\hat{C}_{y,\theta} = e^{-i\theta\sigma_y}$ .

The walker is allowed to move in the direction of the right (left) depending on the outcomes internal state of qubit state after the application of coin operator through the conditioned-shift operator:

$$\hat{S} = |0\rangle\langle 0| \otimes \sum_{x=i}^i |x+1\rangle\langle x| + |1\rangle\langle 1| \otimes \sum_{x=i}^i |x-1\rangle\langle x|. \quad (8)$$

If the internal coin state is  $|0\rangle$  the walker is allowed to move to the right and if the resulting coin operator yields the  $|1\rangle$  the walker moves to the left. This allows the walker to shift in the form of the superposition of position space by iterating this walker via the unitary walk evolution operator of

$$\hat{W}_\theta^N = \hat{S}(\hat{C} \otimes \hat{I}). \quad (9)$$

Without taking any intermediate measurement during the  $N$  steps of iteration, the time evolution of the quantum walker is given:

$$|\Psi(t)\rangle = \hat{W}_\theta^N \Psi(0) = \hat{W}_\theta^N [|\psi\rangle \otimes |x=0\rangle], \quad (10)$$

which yields the superposition of possible path taken by the walker. We shall refer to this type of standard quantum walk as the pure or noiseless DTQW.

### C. Noisy discrete-time quantum walk

The behavior of the DTQW is controlled by the choice of coin operator. Fixing a constant value of coin parameter throughout the entire evolution represents the homogeneous time-evolution DTQW following (10). The inhomogeneity in DTQW either in the temporal or spatial disorder of the QW can lead to broken symmetry of the time translation. In this work, we study the fractal temporal disorder in the DTQW evolution by introducing angle fluctuation using fGn. The angle parameter for the coin operator  $\hat{C}$  is expressed in the form of  $\theta(t) = \theta_0 + \gamma W_H(t)$ , where the  $W_H(t)$  is the fGn, with noise strength parameter,  $\gamma$  (measured in angle), and  $\theta_0$  is a fixed rotation angle that parametrizes the particular quantum walk. The fGn is sampled for each instant of time step  $t$ . The coin operator in this case takes the form of

$$\hat{C} = \begin{bmatrix} \cos[\theta(t)] & \sin[\theta(t)] \\ \sin[\theta(t)] & -\cos[\theta(t)] \end{bmatrix}. \quad (11)$$

The fractal noise will induce fluctuations in rotation of the qubit state due to random coin operation of  $\hat{C} = e^{-i\theta(t)\sigma_y}$  as shown in Fig 1.

When modeling the quantum gate error, this form of fluctuation in the rotations is commonly treated as a classical noise, as compared to the quantum noise resulting from the system-bath interactions that affect the qubit's internal states.

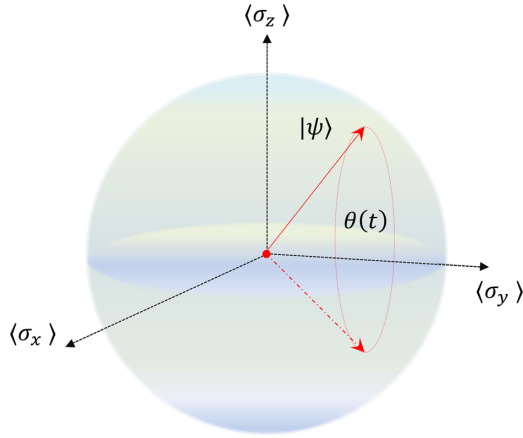


FIG. 1. Fluctuation in the rotation of qubit state due to random coin operation of  $\hat{C} = e^{-i\theta(t)\sigma_y}$ .

The state of the walker after step  $t$  with disorder will be

$$\begin{aligned} |\Psi(t)\rangle &= [\hat{W}_{\theta(t)}]^t (|\psi\rangle \otimes |x=0\rangle) \\ |\Psi_t\rangle &= [\hat{W}_{\theta(t)}]^t |\Psi_{in}\rangle = \hat{W}_x(\theta_t) \dots \hat{W}_x(\theta_3) \hat{W}_x(\theta_2) \hat{W}_x(\theta_1) |\Psi_{in}\rangle \\ &= \hat{S}(\hat{C}(\theta_t) \otimes \hat{I}) \dots \hat{S}(\hat{C}(\theta_3) \otimes \hat{I}) \dots \hat{S}(\hat{C}(\theta_0) \otimes \hat{I}) |\Psi_o\rangle \end{aligned} \quad (12)$$

with randomly chosen coin parameters  $\theta_t \in \{0^\circ, 90^\circ\}$  for each time step. Even though the coin parameter is randomly chosen for each step (iteration), the evolution is still unitary. We shall refer to DTQW with fGn coin as the noisy DTQW with Hurst parameter  $H$ .

In order to verify the performance of protocol for the quantum error correction (QEC) and to characterize quantum hardware requires a realistic laboratory environment. Often most protocols assumed the environmental noise originated from the independent and identically random process. In the physical implementation of the DTQW via the quantum circuit using a physical qubit state, such as the single trapped atom, one may consider the environmental noise modeled as the temporal correlated noise. For instance, long-time correlated noise is likely to occur due to the changes in the electrical apparatus' ambient temperature and duty cycle throughout operations. Meanwhile, the short-time correlated noise arises from the anomalous heating in the ion trap, and uncorrelated white noise is produced by the electrical components [14]. Therefore, fGn is well suited to capture the temporal correlation behavior of fluctuation with different Hurst indices. The application of correlated noise as a source of noise in the randomized benchmarking and gate-set tomography protocol reduced the discrepancy between the theoretical and experimental performance [15].

### III. METHODOLOGY

The simulation of the DTQW is carried out using the QUTIP (Quantum Toolbox on PYTHON) [15,16]. The initial state of the walker is prepared as  $|\Psi_0(0)\rangle = 1/\sqrt{2}(|0\rangle + i|1\rangle) \otimes |x=0\rangle$ . In this work, we assigned a fixed coin parameter  $\theta = 45^\circ$  to produce the Hadamard quantum walk. For the numerical sim-

ulation, the DTQW is evolved up to 200 time steps, sufficient to realize the correlation transfer properties that we wish to highlight in this study. The set of random number representing fGn is simulated using Fourier spectral method with the prescribed power-law spectral density for the selected Hurst parameter (see the Appendix). To capture the correlation of random numbers, we first performed 1000 steps simulation of fGn noise and segmented 200 points from the dataset at 700 steps. This is to ensure the stationarity of fGn as fractal noise with the prescribed Hurst index before being fed into the coin parameter during DTQW evolution. The simulation is repeated with 100 sets of independently generated random numbers representing fGn.

## IV. RESULTS AND DISCUSSION

### A. Weak localization of the walk

The noise strength  $\gamma$  affects the probability distribution of the noisy DTQW after 200 steps of iteration in position space more significantly compared to the variation due to the Hurst parameters as shown in Fig. 2. The walker has a farther spread when the coin parameter is subjected to maximum noise strength of  $\gamma = 45^\circ$ , which allows the qubit state to rotate across the Bloch sphere in the full range of  $0 \leq \theta \leq 45^\circ$ . This pattern is consistent for all the Hurst parameters selected in this study, namely  $H = 0.25$  (antipersistent fGn),  $H = 0.5$  (uncorrelated white noise), and  $H = 0.75$  (persistent fGn). The noiseless DTQW distribution rightfully shows the oscillatory pattern and the expected double peaks near the two ends of the lattice space. These peaks correspond to the ballistic peaks. A small increase in noise strength of  $\gamma = 1^\circ$  yields the same distribution profile. With a further increase in the noise strength  $\gamma = 5^\circ$ , the ballistic peaks shrink and start to merge at the center. The persistent ballistic peaks indicate the weak noise is unable to modify the interference pattern of the walk. When the noise strength is significantly large with  $\gamma = 45^\circ$ , the probability distribution becomes a single localized peak at the center. The temporal noise disorder in the coin parameter modifies the interference patterns of the DTQW, which is reflected in the probability distribution. In general, introducing correlated (both antipersistent and persistent) noises induce weak localization of the DTQW towards the center of the lattice. Further examination of the distributions shows the noisy DTQW with antipersistent fGn has modified the interference pattern of the DTQW more than the persistent and uncorrelated fGn cases.

The broken symmetry of the DTQW evolution due to disorder media or randomized unitary operation can lead to Anderson localization or weak localization depending on the nature of the disorder. A distinct feature of weak localization is the probability distribution profile has slow decay away from the origin, while the probability profile for the Anderson localization shows a fast (exponential) decay. The weak localization produced by the DTQW under randomized unitary operation with the temporal disorder as presented in this work corroborates with what was reported in Refs. [17,18]. The lack of the Anderson localization in the case of temporal disorder DTQW is pointed out by Refs. [6,18] due to the presence of gauge transformation that removes the randomness in the

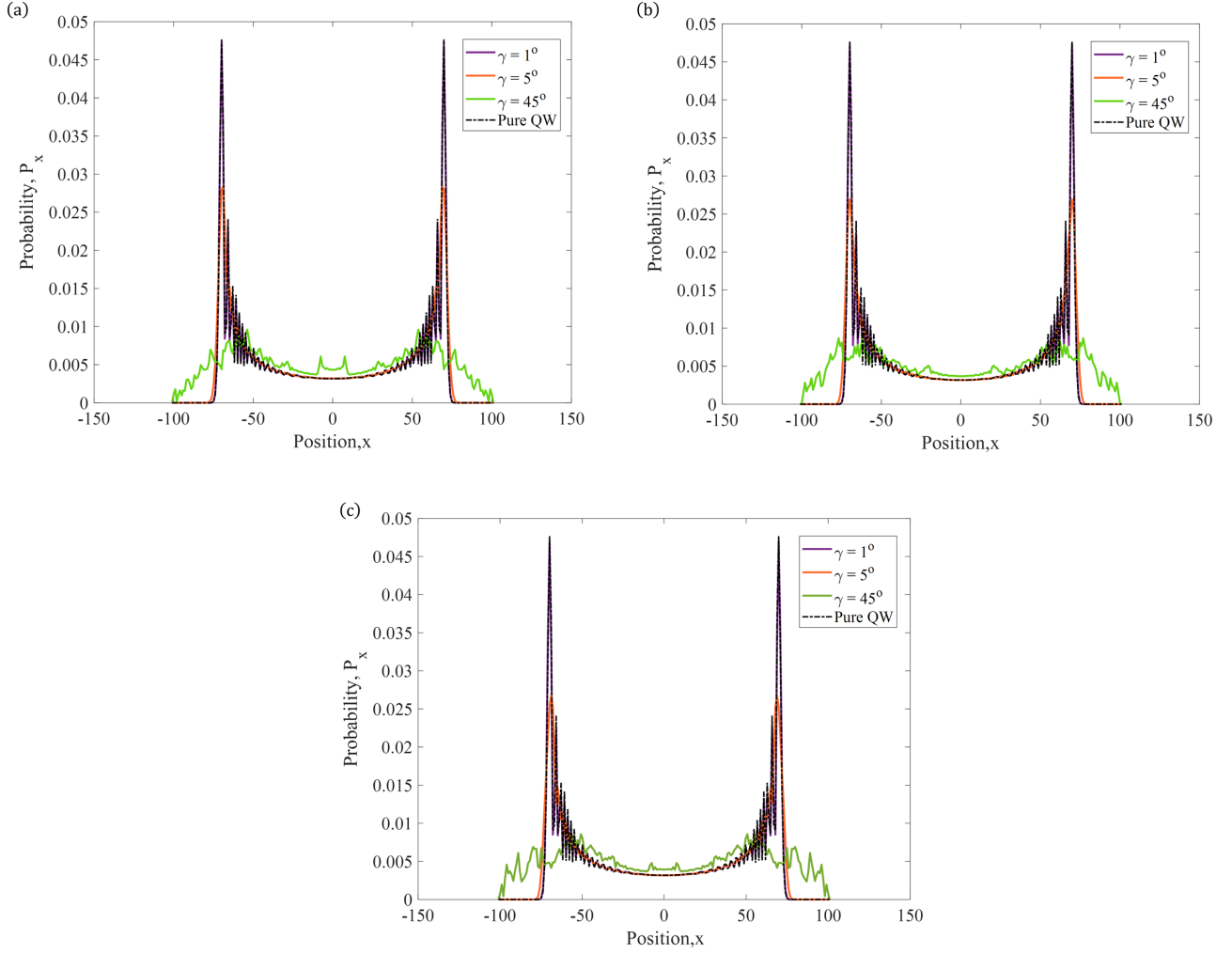


FIG. 2. Probability distributions of noisy DTQW with Hurst exponent (a)  $H = 0.25$ , (b)  $H = 0.50$ , and (c)  $H = 0.75$  with noise strengths:  $\gamma = 1^\circ$  (purple),  $5^\circ$  (orange), and  $45^\circ$  (green) after  $t = 200$ . The black-dashed line represents the distribution of noiseless or pure DTQW. The initial state of the walk is  $1/\sqrt{2}[|0\rangle + i|1\rangle] \otimes |x = 0\rangle$ .

system [19]. Only spatial disorder can induce strong Anderson localization in the DTQW system.

We are tempted to examine the variance of the noisy DTQW to see if the effect of fGn with different  $H$  indices may be further elucidated. The variance of the DTQW is computed using

$$\sigma^2 = \sum_{x=1}^n P_x (x - \mu)^2, \quad (13)$$

with  $P_x$  is the probability of the walk to be located at the site  $x$  and  $\mu$  is the mean position. The variance of the DTQW exhibits power-law scaling behavior with the scaling exponent  $\alpha$ , which can be estimated using linear regression on the bilogarithm variance plot. We observe in Fig. 3(a) that the noisy DTQW for the selected noise strength and Hurst parameters retains its ballistic spread with a scaling exponent of  $\alpha \sim 2$ , just like the case for noiseless DTQW. Apparently, the variance is unable to differentiate the noisy DTQW and noiseless DTQW.

We first examine the Shannon entropy analysis before emphasizing the advantage of von Neumann entropy for investigating the information backflow. Shannon entropy  $S_H$  generated from the probability of event occurrence in the  $n$  microscopic state is defined as

$$S_H = - \sum_{x=1}^n P_x \log_2 P_x. \quad (14)$$

In contrast to the variance analysis that gives the ballistic feature to both noiseless and noisy DTQWs, the Shannon entropy measure is able to differentiate between the two. The noiseless DTQW generates a slightly higher Shannon entropy compared to the noisy DTQW as shown in Fig. 3(b). However, there are no significant differences in the Shannon entropy of the noisy DTQW with respect to the Hurst parameters.

An alternative measure to investigate the localization properties of the DTQW is to compute the inverse participation ratio ( $\mathcal{J}$ ), which is defined as [7]

$$\mathcal{J}(t) = \frac{1}{\sum_x [P_x(t)]^2}, \quad (15)$$

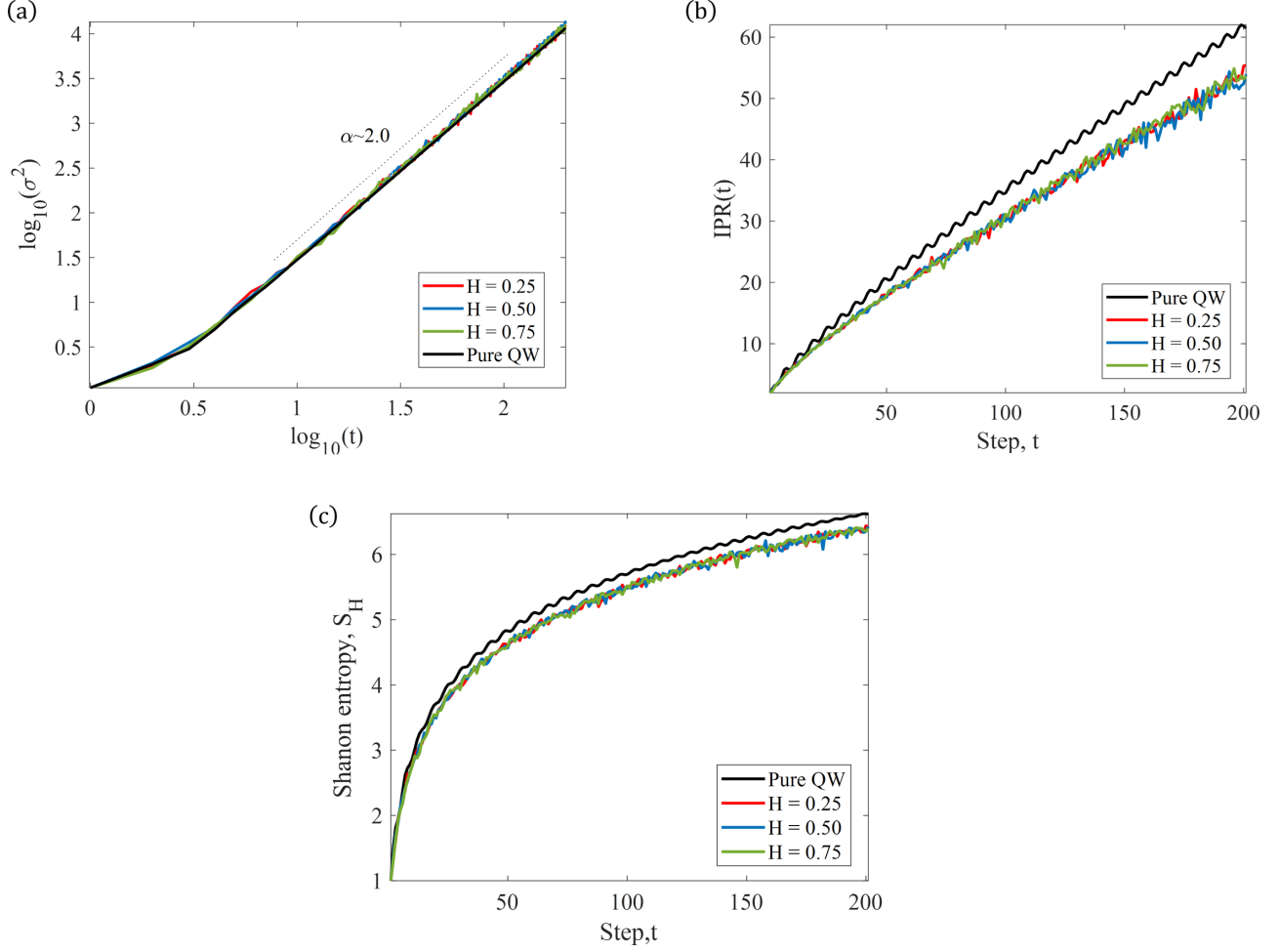


FIG. 3. (a) Bilogarithm variance, (b) Shannon entropy, and (c) inverse participation ratio (IPR) for the noisy DTQW with Hurst exponent  $H = 0.25$  (red),  $H = 0.5$  (blue), and  $H = 0.75$  (green) and noise strength  $\gamma = 45^\circ$ . The noiseless DTQW is plotted in black line.

where  $P_x(t)$  is the probability of finding the walker at sites  $x$  at step time  $t$  with  $P_x(t) = |\Psi_i|^2$ . The IPR measure gives information on the average number of lattice points that the quantum walker spreads over. In Fig. 3(c), the IPR monotonically increased with the number of steps for all the cases and showed a slight difference in the spread between noiseless DTQW and the noisy DTQW. No significant difference is observed among the noisy DTQW with different Hurst parameters. The IPR nevertheless verifies the reduced average lattice points covered by the noisy DTQW as compared to standard DTQW. This difference is also captured in the probability distribution in position space as mentioned earlier.

The IPR, Shannon entropy, and variance generated by the noisy DTQW indexed by the different Hurst parameter of fGn noise, does not show significant variation in the position space. This implies the temporal randomness in the coin parameter has less influence on the walker's dynamics, and thus cannot act as a resource to control the dynamics in position space. It is natural to ask, how does the disorder affect the dynamics of DTQW in the coin space? To answer this question, we compute the quantum entanglement property given by the von Neumann entropy.

## B. Information backflow

The superposition state of the quantum walker and information backflow can be deduced from the entanglement measure between the particle's coin state and position state of DTQW. At the initial step of the evolution, the coin state will be entangled with the walker's position state. The coin operator acts as a manual for the next step of the QW's translation as it controls the extent of the interference in QW. This entanglement between the coin state and position state can be computed using the von Neumann entropy

$$S_{vN} = -\text{Tr}(\rho_c \log_2 \rho_c), \quad (16)$$

where  $\rho_c = \text{Tr}_x(\rho) = \sum_x \langle x | (\Psi_t) \langle \Psi_t | | x \rangle$  is the reduced density matrix obtained by tracing out the position basis  $\rho_x$  from the full composite density matrix  $\rho = |\Psi\rangle\langle\Psi|$  of the DTQW. The general quantum state at any arbitrary step  $t$  is written as

$$|\Psi(t)\rangle = \sum_n (a_x(t)|0\rangle_c + b_x(t)|1\rangle_c) \otimes |x\rangle. \quad (17)$$

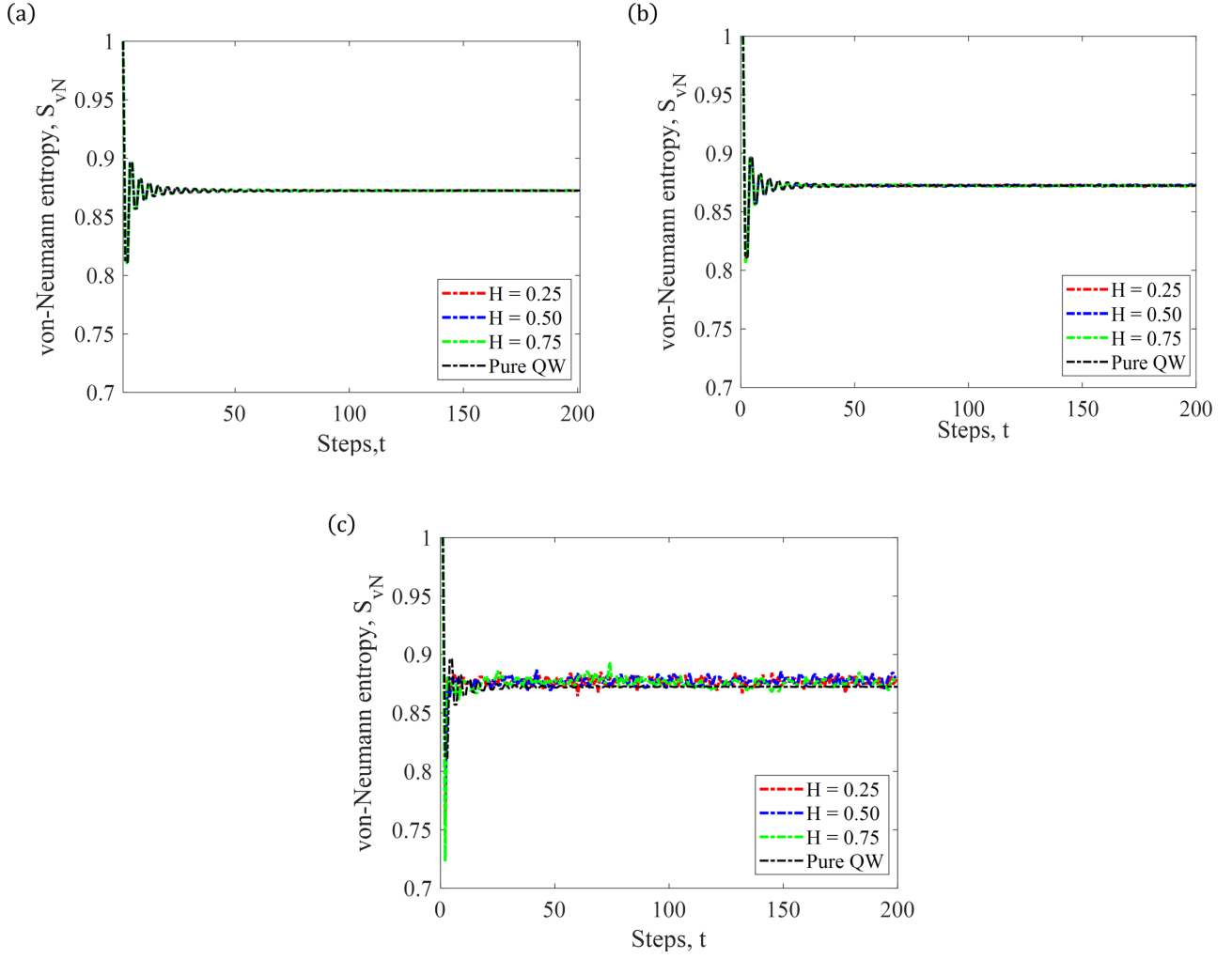


FIG. 4. Degree of entanglement (von Neumann entropy) of the noisy DTQW driven by fGn coin of  $H = 0.25$  (red),  $H = 0.50$  (blue), and  $H = 0.75$  (green) with noise strength of (a)  $\gamma = 1^\circ$ , (b)  $\gamma = 5^\circ$ , and (c),  $\gamma = 45^\circ$ . Entropy of noiseless DTQW is plotted in black line. Asymptotic value for  $S_E(t \rightarrow \infty)$  of the disorder-free Hadamard walk is 0.872 (gray-dashed line).

The time-dependent density matrix of the quantum system is given by

$$\begin{aligned} \rho(t) &= |\Psi(t)\rangle\langle\Psi(t)| \\ &= \sum_{x,x'} (a_x(t)|0\rangle_c + b_x(t)|1\rangle_c)(a_x^*(t)\langle 0| \\ &\quad + b_x^*(t)\langle 1|) \otimes |x\rangle\langle x'|. \end{aligned} \quad (18)$$

The reduced density matrix is then written as

$$\rho_c(t) = \sum_x \langle x|\rho(t)|x\rangle = \sum_m \begin{bmatrix} |a_x(t)|^2 & a_x(t)b_x^*(t) \\ a_x^*(t)b_x(t) & |b_x(t)|^2 \end{bmatrix}, \quad (19)$$

with eigenvalues of [20]

$$\Lambda_{\pm} = \frac{1}{2} \pm \frac{1}{2} \sqrt{1 - 4\Gamma\Omega + 4|\Pi|^2}, \quad (20)$$

where  $\Gamma = \sum_x |a_x(t)|^2$ ,  $\Omega = \sum_x |b_x(t)|^2$ ,  $\Pi = \sum_x a_x(t)b_x^*(t)$ , with  $\Gamma + \Omega = 1$ . Then, the entanglement expression

becomes

$$S_{vN}(t) = -\Lambda_+ \log_2 \Lambda_+ - \Lambda_- \log_2 \Lambda_-. \quad (21)$$

The level of entanglement between the internal (coin) and external (position) degree of freedom over the time evolution of bipartite system is shown in Fig. 4.

At the initial condition, the quantum walk starts from a state with minimum entropy  $S_{vN} = 0$  and it corresponds to a separable state, where the state of the walker is known with certainty. At noise strength  $\gamma = 1^\circ$  [Fig. 4(a)] and  $\gamma = 5^\circ$  [Fig. 4(b)], we observed no significant difference between the standard noiseless DTQW and the noisy DTQW with fGn coin. For the noiseless DTQW, the dashed black horizontal line shows the asymptotic entanglement entropy of  $S_{vN} \rightarrow 0.872$  as obtained in Ref. [21]. As we increase the noise strength to  $\gamma = 45^\circ$ , which allows the coin parameter to fluctuate between  $0^\circ \leq \theta \leq 90^\circ$ , we observe a significant enhancement of the entanglement at the limit of long time as shown in Fig. 4(c). For all the cases of noisy DTQW with fGn of  $H = 0.25$ ,  $H = 0.5$ , and  $H = 0.75$ , the  $S_{vN}$  shows an increment implying that the coin becomes more entangled to

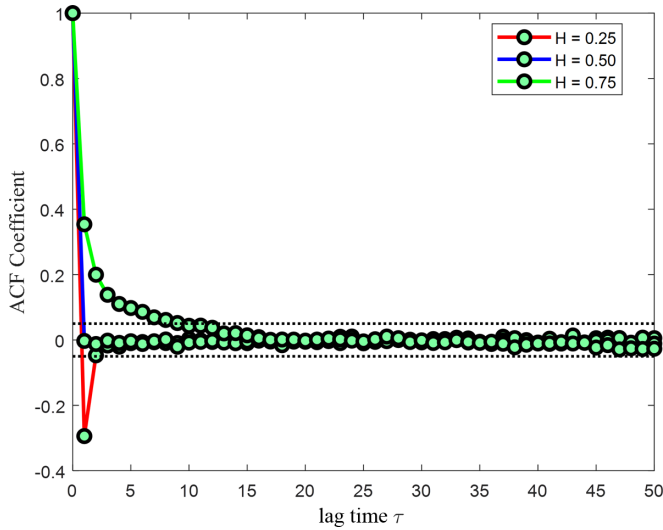


FIG. 5. Autocorrelation function of fractional Gaussian noise for  $H = 0.25$  (red line),  $H = 0.50$  (blue line), and  $H = 0.75$  (green line).

position, hence the slightly higher production of entanglement compared to the disorder-free case. Similar enhanced entanglement has also been shown in Ref. [20].

We observe the so-called information backflow deduced from the von Neumann entropy of the noisy DTQW at the noise of strength of  $\gamma = 1^\circ$  and  $\gamma = 5^\circ$ . The von Neumann entropy exhibits an oscillatory pattern at early iteration steps before the value stabilizes at larger steps. This oscillatory pattern is attributed to the strong presence of memory-effect marking information backflow between the coin and position degree of freedom at the early step of the walk. At the maximum noise level,  $\gamma = 45^\circ$ , we observed the fluctuation of the entropy throughout the evolution [Fig. 4(c)]. This fluctuation is not noticeable at other noise levels. The interaction between the degree of freedoms of the coin and position states in the DTQW system creates quantum memory, which can be identified via the backflow of information. The presence of the backflow information is required to maintain the entanglement in the quantum system [22]. The backflow of information from the environment (position) back to the system (coin) implies that the information on the previous state of system can be stored in the quantum correlation between the system and environment. As pointed out in Ref. [6], the memory effects of the DTQW increased under temporal disorder.

In this work, we conjecture that a quantum system can inherit the correlation of the classical noise imposed to the system and this may be traceable in some relevant quantities, such as the von-Neumann entropy fluctuation. To gain insight on the state of qubit information memory, we calculate the autocorrelation function of the von-Neumann entropy fluctuation.

### C. Correlation transfer

The comparison of the von Neumann entropy generated by the noisy DTQW with fGn of different Hurst indices at a particular noise level does not yield any significant difference. Does this imply that the fGn cannot act as a resource to control

the dynamics of DTQW in the coin and position space? The fGn noise is injected into the coin parameter; logically, we expect to see some behavioral change in the noisy DTQW compared to the standard DTQW. Correlation transfer has been previously considered for the case of displaced Brownian particle in the fluid in which memory effect is added onto the particle's motion due to hydrodynamic information backflow of the environment [23]. Taking inspiration from this phenomenon, we analyze the “memory” kernel of the quantum coin by evaluating the autocorrelation of the von Neumann entropy to see whether the transfer of correlation from the noisy coin state is traceable in the DTQW system. The evaluation of the von Neumann entropy (21) is based on the eigenvalues of the reduced coin-density matrix  $\rho_c$ , which carries the information about the dynamics of the coin state and thus, can be used in the evaluation of memory inheritance in noisy DTQW.

The autocorrelation function (ACF) is often used to determine the presence of memory effect or long-range dependence in the time series. The ACF trend for antipersistent of fGn ( $H = 0.25$ ) shows negative correlation at the early lag time before it bounces back to almost zero correlation at a later time. The ACF quickly decorrelates as the correlation among neighborhood points rapidly reduces, even at small shifts of signal with respect to itself. This noise has a poor memory of its past values, reminiscent of a short-memory stochastic process. The uncorrelated fGn ( $H = 0.5$ ) shows zero correlation at all lag times as the random signal at one particular time is completely uncorrelated with the next instant. The noise originating from a long-memory process such as the persistent fGn ( $H = 0.75$ ) exhibits positive correlation at the early lag time before slowly decaying to zero at large lag time. These three different correlation behaviors are shown in Fig. 5.

The ACF of the von Neumann entropy fluctuation for noisy DTQW with fGn of different Hurst indices and noise strengths are shown in Fig. 6. For noiseless DTQW (gray line) in Fig. 6, the ACF of the von Neumann entropy fluctuation oscillates and decays in amplitude as the lag increases. The ACFs of noisy DTQW (red line) for the three regimes of Hurst indices with noise strength of  $\gamma = 1^\circ$  [Fig. 6(a)] inhibit a similar oscillatory profile in phase with the noiseless DTQW (gray line) but with reduced amplitude. For this case, the ACF trends do not mirror the correlation trend of the fGn (blue-dashed line). This is a manifestation of the periodic cycle in the evolution of entanglement between coin and position. The values of each peak happened at the same lag indices of symmetry and regularity of von Neumann entropy (see Fig. 4). The maximum peak of the ACF's profile occurs at lag shift of 4, 8, 12, ... Then, the maximum and minimum degrees of entanglement between coin and position repeat themselves within the period of 4 and 8.

However, when we increase noise strength to  $\gamma = 5^\circ$  [Fig. 6(b)] and  $\gamma = 45^\circ$  [Fig. 6(c)] (which allows the coin parameter to swing the qubit state in the range of  $40^\circ \leq \theta \leq 50^\circ$  and  $0^\circ \leq \theta \leq 90^\circ$ , respectively), we do not observe any clear oscillatory trend in the ACF, which indicates the lack of periodicity in the von Neumann entropy. Instead, the ACF of the von Neumann entropy fluctuation is now mimicking the ACF of the fGn noise, as the entanglement of QW takes

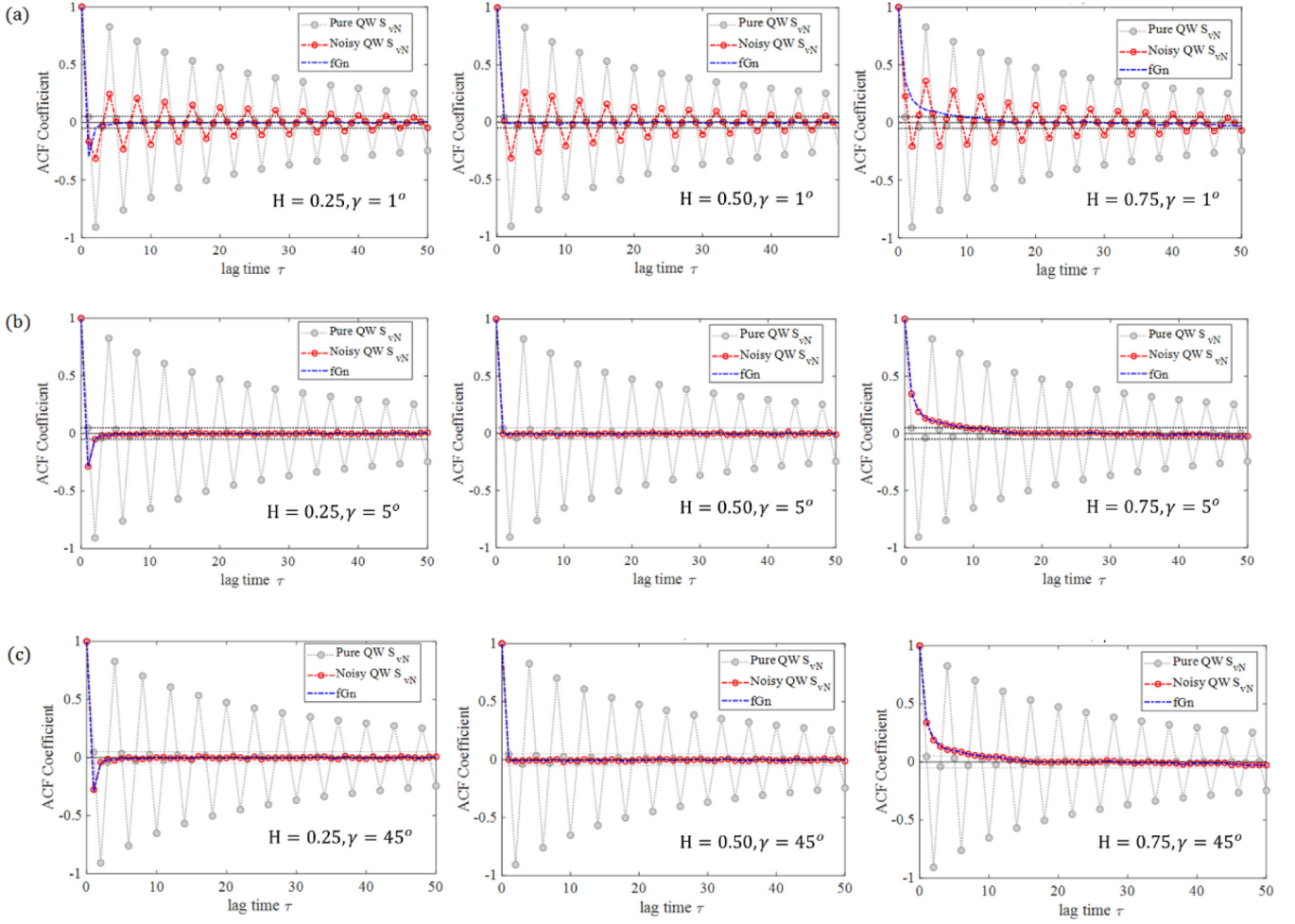


FIG. 6. Autocorrelation function of the von Neumann entropy fluctuation (red line) for noisy DTQW fGn ( $H = 0.25$ ,  $H = 0.5$ , and  $H = 0.75$ ) with noise strength of (a)  $\gamma = 1^\circ$ , (b)  $\gamma = 5^\circ$ , and (c)  $\gamma = 45^\circ$  averaged over 100 samples of DTQW (200 steps) simulation, shown in comparison to fGn (blue line) and noiseless DTQW (gray line).

the pattern of the injected noise. Interestingly, the ACFs of the disorder DTQW perfectly overlap the ACF of the fGn. There appeared to be a correlation transfer from the fGn to the von Neumann entropy fluctuation in the noisy DTQW. This fractal noise correlation transfer has not been reported in the literature and requires further investigations. An example of noise correlation transfer was reported in Ref. [24], where the pure dephasing noise assists the inheritance of correlation in entangled qubits from one position to the next position without sacrificing the coherence of the entangled qubit state.

The transfer of temporal noise correlation in DTQW may enhance the information backflow and entanglement in the disorder DTQW system as shown in Refs. [6,18,20]. The memory effects arising from the temporal noise added to the DTQW system are captured by the ACF of the entropy fluctuation. The von Neuman entropy fluctuation, which could have been easily discarded as a noisy artifact of maximum noise strength, actually provides some insights on the information backflow from the noisy coin state to the position space. During the unitary evolution of the DTQW, the qubit state acts as an information carrier, where it extracts more information from the position measurement outcome [25]. At the

same time, the position space acts as the information storage [26]. Through the backward iterative analysis in Ref. [26], it was shown that the stored information can be perfectly recovered at specific periodic step  $t$ , which is in line with the ACF profile of the DTQW. With added temporal disorder, the retrieval of information is made to be independent of step, i.e., in principle, one can perfectly recover the information of the qubit state stored in the position step on demand. The reason behind this is the position space temporarily stores the information on the coin's initial state and then this information flows back from the environment, reminding the system of its past. The gain of information from the system to the environment induces the restoration of the system's initial state which strengthens entanglement.

## V. CONCLUSION

In this work, we have studied the behaviors of DTQW with random coin parameters driven by fractional Gaussian noise with different Hurst indices and noise strengths. The presence of correlated (antipersistent and persistent) noises induces weak localization of the DTQW towards the center



of the lattice as observed from the distribution function. The subtle correlation effects of the fGn-driven coin were not clearly observed in the variance and the Shannon entropy. The von Neumann entropy has more to offer in elucidating the correlation transfer from the coin parameters to the dynamics of the noisy DTQW. This result may be useful for manipulating noise correlation as a resource to sustain and manipulate information backflow via the interaction of a quantum system with a noisy environment. For instance, the localization of QW at finite position space, which is linked to enhancing information backflow, can be utilized as a secure way to store the information of the qubit state because the eavesdropper does not have information on the full position space [14]. The coin state of the DTQW system is effectively sensitive to the relatively weak disorder. We showed the ACF of the qubit's von Neumann entropy fluctuation overlapped almost perfectly on the ACF of the fGn's allowing the noisy DTQW to extract the spectral content of weak environmental noise. This finding may be useful in integrating the DTQW as a sensor of noise in the quantum noise spectroscopy (QNS) protocol [27,28]. Additionally, the transfer of classical noise correlation into the coin state opens a possibility to perform an indirect probe

of the qubit state, in contrast to a direct measurement of the quantum state which will cause the wave function to collapse.

**ACKNOWLEDGMENT**

This work is supported by the Malaysian Ministry of Higher Education Fundamental Research Grant Scheme (Grant No. FRGS/1/2020/STG07/UM/01/2).

**APPENDIX: SIMULATION OF fGn USING SPECTRAL SYNTHESIS METHOD**

A stationary fractal stochastic process  $X(t)$  such as the fGn with a known Hurst exponent can be generated by using the spectral synthesis method [29,30] from its power spectral density  $S(f)$ , namely,

$$S(f) \propto \frac{1}{f^\beta}, \tag{A1}$$

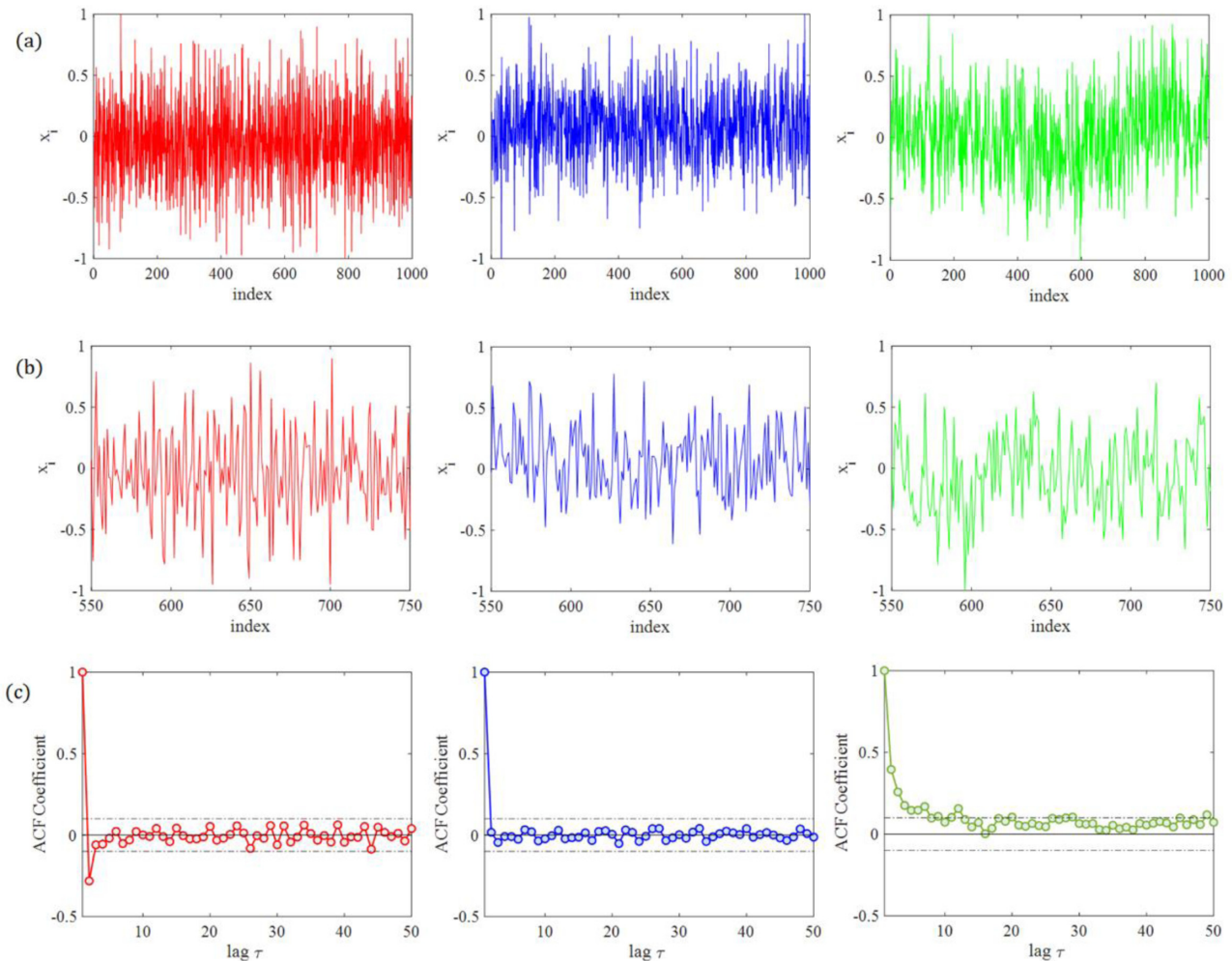


FIG. 7. Sample of the generated fractional Gaussian noise for 1000 steps (a); with 2200 resample points (b); and the ACF (c) for different values of the Hurst exponent  $H = 0.25$  (red),  $0.50$  (blue), and  $0.75$  (green).

with  $\beta = 2H - 1$ . The square modulus of Fourier transforms of the signal  $X(f)$  is written as the power spectral density:

$$S(f) = |X(f)|^2 \propto f^{-\beta}. \quad (\text{A2})$$

The complex series of  $X(f)$  with modulus  $r(f)$  proportional to  $1/f^{\beta/2}$  is obtained via the relationship

$$r(f) = \frac{W_{Gn}(f)}{f^{\beta/2}}, \quad (\text{A3})$$

where  $W_{Gn}$  is Gaussian white noise with frequency  $f$ . To draw a random phase  $\phi$  for the complex series, the white noise with uniform distribution  $W_{un}$  is used:

$$\phi = 2\pi W_{un}, \quad (\text{A4})$$

and complex coefficient is obtained via

$$a(f) = r(f) \cos \phi(f), \quad b(f) = r(f) \sin \phi(f), \quad (\text{A5})$$

Then, the complex series  $S(f)$  is generated as =

$$X(f) = a(f) + ib(f). \quad (\text{A6})$$

Finally, the inverse Fourier transform is applied to  $X(f)$  to obtain time-series domain of the fGn:

$$X(t) = \mathbb{F}^{-1}\{X(f)\} = \frac{1}{N} \sum_{f=1}^N X(f) e^{i2\pi f(t/N)}, \quad (\text{A7})$$

with  $t = 1, 2, 3, \dots$  for  $N$  finite sequence. The three different values of Hurst exponent  $H = 0.25, 0.50, \text{ and } 0.75$ , respectively, are used to generate the 1000 steps of fGn signals as shown in Fig. 7(a). From the 1000 steps, we segmented 200 points from 550 to 750 steps [Fig. 7(b)] as the input random number in DTQW evolution. To ensure the generated fGn corresponds to the behavior associated with the input Hurst exponent, we further compute the ACF of the noise as shown in Fig. 7(c).

- 
- [1] B. Bellomo, R. Lo Franco, and G. Compagno, Non-Markovian Effects on the Dynamics of Entanglement, *Phys. Rev. Lett.* **99**, 160502 (2007).
- [2] S. Maniscalco, F. Francica, R. L. Zaffino, N. Lo Gullo, and F. Plastina, Protecting Entanglement Via the Quantum Zeno Effect, *Phys. Rev. Lett.* **100**, 090503 (2008).
- [3] S. F. Huelga, Á. Rivas, and M. B. Plenio, Non-Markovianity-Assisted Steady State Entanglement, *Phys. Rev. Lett.* **108**, 160402 (2012).
- [4] Y. Dong, Y. Zheng, S. Li, C. C. Li, X. D. Chen, G. C. Guo, and F. W. Sun, Non-Markovianity-Assisted high-fidelity Deutsch–Jozsa algorithm in diamond, *Npj Quantum Inf.* **4**, 1 (2018).
- [5] C. Addis, G. Brebner, P. Haikka, and S. Maniscalco, Coherence trapping and information backflow in dephasing qubits, *Phys. Rev. A: At. Mol. Opt. Phys.* **89**, 024101 (2014).
- [6] N. P. Kumar, S. Banerjee, and C. M. Chandrashekar, Enhanced non-Markovian behavior in quantum walks with Markovian disorder, *Sci. Rep.* **8**, 8801 (2018).
- [7] J. Han, Z. Li, J. Zhang, H. Xu, K. Linghu, Y. Li, C. Li, M. Chen, Z. Yang, J. Wang, T. Ma, G. Xue, Y. Jin, and H. Yu, Characterizing noise correlation and enhancing coherence via qubit motion, *Fundam. Res.* **1**, 10 (2021).
- [8] M. A. C. Rossi, C. Benedetti, M. Borrelli, S. Maniscalco, and M. G. A. Paris, Continuous-time quantum walks on spatially correlated noisy lattices, *Phys. Rev. A* **96**, 040301(R) (2017).
- [9] B. B. Mandelbrot and J. W. van Ness, Fractional Brownian motions, fractional noises and applications, *SIAM Rev.* **10**, 422 (1968).
- [10] H. Qian, Fractional Brownian Motion and Fractional Gaussian Noise, in *Processes with Long-Range Correlations: Theory and Applications*, edited by G. Rangarajan and M. Ding (Springer, Berlin, 2003), Vol. 621, pp. 22–33.
- [11] D. Koutsoyiannis, The Hurst phenomenon and fractional Gaussian noise made easy, *Hydrol. Sci. J.* **47**, 573 (2002).
- [12] G. Shevchenko, Fractional Brownian motion in a nutshell, *Int. J. Mod. Phys. Conf. Series*, **36** 1560002 (2015).
- [13] M. A. Riley, S. Bonnette, N. Kuznetsov, S. Wallot, and J. Gao, A tutorial introduction to adaptive fractal analysis, *Front. Physiol.* **3**, 1 (2012).
- [14] C. D. Wilen, S. Abdullah, N. A. Kurinsky, C. Stanford, L. Cardani, G. D’Imperio, C. Tomei, L. Faoro, L. B. Ioffe, C. H. Liu, A. Opremcak, B. G. Christensen, J. L. DuBois, and R. McDermott, Correlated charge noise and relaxation errors in superconducting qubits, *Nature (London)* **594**, 369 (2021).
- [15] S. Mavadia, C. L. Edmunds, C. Hempel, H. Ball, F. Roy, T. M. Stace, and M. J. Biercuk, Experimental quantum verification in the presence of temporally correlated noise, *Npj Quantum Inf.* **4**, 387 (2018).
- [16] J. R. Johansson, P. D. Nation, and F. Nori, QuTiP: An open-source python framework for the dynamics of open quantum systems, *Comput. Phys. Commun.* **183**, 1760 (2012).
- [17] C. M. Chandrashekar, Disorder induced localization and enhancement of entanglement in one- and two-dimensional quantum walks, [arXiv:1212.5984](https://arxiv.org/abs/1212.5984) [quant-ph].
- [18] N. Konno, One-dimensional discrete-time quantum walks on random environments, *Quantum Inf. Process.* **8**, 387 (2009).
- [19] A. Joye and M. Merkli, Dynamical localization of quantum walks in random environments, *J. Stat. Phys.* **140**, 1025 (2010).
- [20] M. Zeng and E. H. Yong, Discrete-time quantum walk with phase disorder: Localization and entanglement entropy, *Sci. Rep.* **7**, 12024 (2017).
- [21] O. Maloyer and V. Kendon, Decoherence versus entanglement in coined quantum walks, *New J. Phys.* **9**, 87 (2007).
- [22] N. Mirkin, P. Poggi, and D. Wisniacki, Information backflow as a resource for entanglement, *Phys. Rev. A* **99**, 062327 (2019).
- [23] T. Franosch, M. Grimm, M. Belushkin, F. Mor, G. Foffi, L. Forró, and S. Jeney, Resonances arising from hydrodynamic memory in Brownian motion - The colour of thermal noise, *Nature (London)* **478**, 85 (2011).
- [24] T. Nakajima, M. R. Delbecq, T. Otsuka, S. Amaha, J. Yoneda, A. Noiri, K. Takeda, G. Allison, A. Ludwig, A. D. Wieck, X. Hu, F. Nori, and S. Tarucha, Coherent transfer of electron spin correlations assisted by dephasing noise, *Nat. Commun.* **9**, 2133 (2018).

- [25] B. Kollár, *Disorder and Entropy Rate in Discrete Time Quantum Walks* (University of Pécs, Pécs, Hungary, 2014).
- [26] C. M. Chandrashekar and T. Busch, Localized quantum walks as secured quantum memory, *Europhys. Lett.* **110**, 10005 (2015).
- [27] P. Szańkowski, G. Ramon, J. Krzywda, D. Kwiatkowski, and L. Cywiński, Environmental noise spectroscopy with qubits subjected to dynamical decoupling, *J. Phys.: Condens. Matter* **29**, 333001 (2017).
- [28] T. Chen, X. Zhang, and X. Zhang, Quantum sensing of noises in one and two dimensional quantum walks, *Sci. Rep.* **7**, 4962 (2017).
- [29] R. F. Voss, Fractals in Nature: From Characterization to Simulation, in *The Science of Fractal Images*, edited by H. Peitgen and S. Saupe (Springer, New York, 1988), pp. 21–70.
- [30] C. Roume, S. Ezzina, H. Blain, and D. Delignieres, Biases in the simulation and analysis of fractal processes, *Comput. Math. Methods Med.* **2019**, 12 (2019).